

# PHOTOMETRIC REDSHIFT OF THE GRB 981226 HOST GALAXY

L. CHRISTENSEN<sup>1</sup>

Astrophysikalisches Institut Potsdam, An der Sternwarte 16, 14482 Potsdam, Germany

J. HJORTH<sup>2</sup>

Dark Cosmology Centre, Niels Bohr Institute, University of Copenhagen, Juliane Maries Vej 30, DK-2100 Copenhagen, Denmark

AND

J. GOROSABEL<sup>3</sup>

Instituto de Astrofísica de Andalucía, IAA-CSIC, P.O. Box 03004, E-18080 Granada, Spain

*Draft version June 26, 2021*

## ABSTRACT

No optical afterglow was found for the dark burst GRB 981226 and hence no absorption redshift has been obtained. We here use ground-based and space imaging observations to analyse the spectral energy distribution (SED) of the host galaxy. By comparison with synthetic template spectra we determine the photometric redshift of the GRB 981226 host to be  $z_{\text{phot}} = 1.11 \pm 0.06$  (68% confidence level). While the age-metallicity degeneracy for the host SED complicates the determination of accurate ages, metallicity, and extinction, the photometric redshift is robust. The inferred  $z_{\text{phot}}$  value is also robust compared to a Bayesian redshift estimator which gives  $z_{\text{phot}} = 0.94 \pm 0.13$ . The characteristics for this host are similar to other GRB hosts previously examined. Available low resolution spectra show no emission lines at the expected wavelengths. The photometric redshift estimate indicates an isotropic energy release consistent with the Amati relation for this GRB which had a spectrum characteristic of an X-ray flash.

*Subject headings:* galaxies: distances and redshifts – galaxies: high-redshift – galaxies: starburst – gamma rays: bursts

## 1. INTRODUCTION

The Swift satellite (Gehrels et al. 2004) promises the build-up of a significant sample of gamma-ray bursts (GRBs) with well-understood selection criteria useful for cosmological studies of high-redshift galaxies (Jakobsson et al. 2005) and the Hubble diagram (Ghirlanda et al. 2004a). The best way of securing GRB redshifts is from absorption line studies of the afterglow. However, for the first 56 Swift GRBs only 11 redshifts have been obtained. Alternatively, redshifts can be obtained from host galaxy spectroscopy although this requires that the host is sufficiently bright and has detectable emission lines.

In this Letter we explore a third approach suitable for fainter host galaxies in case a spectroscopic absorption or emission line redshift has not been obtained. For a sample of 10 GRB host galaxies with spectroscopic redshifts in the range  $0.4 < z < 2$  and photometric measurements in more than 4 bands, Christensen et al. (2004a) found that photometric redshifts were consistent with the spectroscopic redshifts in all cases, within  $\Delta z = 0.21$ . An advantage of the method is that it is independent of whether the host galaxy has emission lines.

As the next step in validating the photometric redshift approach we here predict a redshift from a host galaxy with multiband photometry which is sufficiently bright that a spectroscopic redshift can be measured, and thereby test the photometric redshift. Our target

is GRB 981226 which is currently one of the brightest hosts without a spectroscopic redshift.

GRB 981226 was detected by the BeppoSAX satellite on 1998 December 26.41 UT. It is consistent with being an X-ray flash (XRF) with the fluences satisfying  $S_X > S_\gamma$  (Frontera et al. 2000). Despite intense optical and near-infrared (IR) follow-up observations initiated 6.5 and 8.4 hours after the burst, respectively (Klose 1998; Castro-Tirado et al. 1998) no optical counterpart was found (Galama et al. 1998; Wozniak 1998; Rhoads et al. 1998; Bloom et al. 1998; Schaefer et al. 1998). The deep  $R$ -band observations carried out by Lindgren et al. (1999) showed  $R > 23$  mag at 9.9 hours after the GRB. This makes GRB 981226 a typical GRB without any detected afterglow (Taylor et al. 1998) and close to being a dark burst (Jakobsson et al. 2004; Rol et al. 2005).

Radio observations revealed a variable source at the position R.A.(J2000)= $23^h 29^m 37^s.21$ , Dec(J2000)= $-23^\circ 55' 53''.8$  peaking  $\sim 10$  days after the gamma-ray event (Frail et al. 1999). Identification of the host galaxy was suggested based on the small angular separation between the radio afterglow and an extended object. High spatial resolution images from the HST/STIS show that the galaxy colours change notably over its surface, with the northern part being significantly bluer (Holland 2000). The position of the radio afterglow with respect to the galaxy is  $0''.749 \pm 0''.328$  (Bloom et al. 2002), which encompasses the blue northern part of the host.

This Letter presents an analysis of all imaging data on the host available in public archives. Ground-based data in the  $BVRIJsKs$  bands and images from the HST makes

Electronic address: lchristensen@aip.de  
 Electronic address: jens@astro.ku.dk  
 Electronic address: jgu@iaa.es

TABLE 1  
LOG OF THE OBSERVATIONS

Instrument+filter	date	exp time (s)
FORS1 <i>R</i>	2000-10-05	18×540
FORS1 <i>B</i>	2001-05-15	3×300
FORS1 <i>V</i>	2001-05-16	3×300
FORS1 <i>R</i>	2001-06-19	6×540
FORS1 <i>I</i>	2001-05-16	3×300
FORS1 <i>I</i>	2001-08-13	400
FORS1 <i>I</i>	2001-08-19	400
FORS1 <i>I</i>	2001-09-22	4×600
ISAAC <i>Js</i>	2001-09-22	10×180
ISAAC <i>Ks</i>	2000-11-12	30×120
ISAAC <i>Ks</i>	2001-06-07	30×120
STIS <i>CL</i>	2000-07-03	8265 <sup>a</sup>
STIS <i>LP</i>	2000-07-06	7909 <sup>a</sup>

<sup>a</sup>Total integration time.

a multi-wavelength study appropriate to determine the host and hence the GRB photometric redshift. Some of the data have been presented previously in the literature in different contexts. An ISAAC *Ks* band image was presented in Le Floc'h et al. (2003), the HST/STIS data in Holland (2000), and a deep *R* band image in Frail et al. (1999); the latter image is not analysed here.

## 2. DATA ANALYSIS

For consistency we re-analysed the photometry in all filters. The host galaxy was observed in the optical (*BVRI*) with VLT/FORS1 and in the near-IR (*Js* and *Ks*) with ISAAC. The data were retrieved from ESO's public archive<sup>1</sup>. To take advantage of all available data on the host we also included images from the Hubble Space Telescope using STIS. The host was observed in July 2000, using a clear aperture (50CCD, or *CL* filter) and a long pass imaging filter, F28×50LP (*LP* filter)<sup>2</sup>. Table 1 lists the dates of observations, number of integrations and exposure times.

Data reduction was done using IRAF. All optical data were reduced using standard methods, i.e. bias subtraction and dividing by a combined average flat-field frame obtained from twilight sky exposures. For the near-IR data reduction, sky subtraction was done by creating a sky image from the bracketing 8 frames from each individual night. After sky subtraction each image was divided by a normalised flat-field frame. Near-IR flat-field images were created by subtracting faintly illuminated flat-field frames from bright ones. Eight and ten of such images were combined and used for flat-fielding the *Js* and *Ks* images, respectively. Relative shifts were found using cross-correlation procedures before combining the individual exposures.

Additional archive calibration files consisting of bias, sky flat-field, and standard star images from the different nights were retrieved. Photometric zero-points from ISAAC and FORS1 were obtained by comparing the instrumental magnitude of the standard star with tabulated values. All the zero-points calculated confirmed the

TABLE 2  
HOST GALAXY MAGNITUDES

Filter	$m_{\text{Vega}}(\text{mag})$	$m_{\text{AB}}(\text{mag})$
<i>B</i>	25.74±0.37	25.68±0.37
<i>V</i>	25.59±0.15	25.63±0.15
<i>R</i>	24.81±0.06	25.04±0.06
<i>I</i>	23.65±0.15	24.09±0.15
<i>Js</i>	21.90±0.20	22.84±0.20
<i>Ks</i>	21.10±0.27	22.97±0.27
<i>CL</i>		24.79±0.10
<i>LP</i>		24.27±0.10

NOTE. — Magnitudes of the host in the Vega and AB systems in various filters obtained with an aperture radius of 2". No correction for Galactic extinction is applied.

values for the given dates that were found in the corresponding instrument web-pages. Extinction and colour terms are reported for each month on the FORS1 web page and were assumed to be appropriate here. For the STIS data, zero-points were obtained from the STIS user manual.

Aperture photometry was used to derive host photometry, and all magnitudes of the host listed in Table 2 were derived using a 2" radial aperture. Corrections to larger apertures were found to be negligible. No optical afterglow was found for this burst and the observations were carried out 1.5–2.5 years after the burst. Therefore, no contamination of any significant level is expected for the photometry of the host. The magnitudes derived here are consistent with  $R = 24.85 \pm 0.06$  mag in Frail et al. (1999),  $Ks = 21.1 \pm 0.2$  mag in Le Floc'h et al. (2003), and  $CL = 25.04 \pm 0.07$  mag in Holland (2000) (using the same 1"1 radial aperture we find  $25.00 \pm 0.05$  mag).

## 3. PHOTOMETRIC REDSHIFT

We used the public photometric redshift code HyperZ (Bolzonella et al. 2000) along similar lines as in a series of papers on GRB host galaxies (Gorosabel et al. 2003a,b; Christensen et al. 2004b; Gorosabel et al. 2005). As shown in these papers, photometric redshifts of GRB hosts can be determined to within  $\Delta z = 0.21$  when multi-band observations are available, and when spectral features such as the Balmer jump are bracketed by the observations.

Magnitude offsets between Vega and the AB system were calculated and added to the observed Vega magnitudes listed in Table 2. The HST magnitudes are obtained directly in the AB system (see STIS Instrument Handbook), so the Table 2 fields corresponding to the HST Vega magnitudes are empty. To derive fluxes for the various pass bands the magnitudes were corrected for a Galactic extinction of  $E(B-V) = 0.022$  mag as derived from the dust maps of Schlegel et al. (1998). Flux densities in  $\mu\text{Jy}$  were calculated by  $f_\nu = 10^{-0.4(m_{\text{AB}} - 23.9)}$  for an AB magnitude,  $m_{\text{AB}}$ , in each passband.

Fluxes were compared to galaxy template spectra created from the spectral atlas of Bruzual & Charlot (1993). We used different galaxy templates obtained from a Salpeter initial mass function (IMF) (Salpeter 1955) (Sp55) and a Miller & Scalo IMF (Miller & Scalo 1979) (MiSc79) with different star formation histories and a

<sup>1</sup> <http://archive.eso.org>

<sup>2</sup> Images were obtained from [http://www.ifa.au.dk/~hst/grb\\_hosts/intro.html](http://www.ifa.au.dk/~hst/grb_hosts/intro.html) (Holland 2001). The data are part of the Cycle 9 programme GO-8640 "A Public Survey of Host Galaxies of Gamma-ray Bursts".

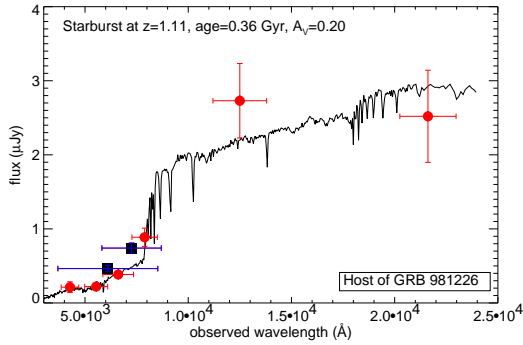


FIG. 1.— Best fit synthetic spectrum to the SED of the GRB 981226 host galaxy using the ground based *BVRJIsKs* images. The template was created from a Sp55 IMF and a Calzetti extinction law. The broad STIS filters are indicated by the squares, but are not included in the fit. Horizontal error bars indicate the widths of each band.

characteristic timescale  $\tau$ , where  $\tau = 0$  corresponds to a starburst template, and  $\tau \rightarrow \infty$  to an irregular galaxy template. Values of  $\tau$  in between these extremes correspond to various types of spiral galaxy and elliptical templates. These templates all assume solar metallicity. We also experimented using different extinction curves: a starburst extinction curve (Calzetti et al. 2000), a Small Magellanic Cloud (SMC) extinction curve (Prevot et al. 1984), a Large Magellanic Cloud (LMC) extinction curve (Fitzpatrick 1986), and the Milky Way extinction curve (Seaton 1979).

In principle the STIS wide filters might be included to determine the photometric redshift. The *CL* filter extends from 4000 to 9000 Å and the *LP* from 5500 to 9000 Å, thus providing poor spectral information. Furthermore given the widths of the filters, the effective wavelength is sensitive to the assumed spectral template. Thus, as a first step, we decided to not include them in our analysis, and then discuss the impact that their inclusion has on the  $z_{\text{phot}}$  determination.

The best fit of the broad band SED was found with a starburst template at  $z = 1.11$  with an age of 0.36 Gyr and an intrinsic extinction of  $A_V = 0.20$  mag as shown in Fig. 1. Using a Calzetti extinction curve and a Sp55 IMF gave the smallest reduced  $\chi^2/\text{d.o.f.}$  as indicated in Table 3. Other combinations of template fits are also listed in Table 3. In all cases a starburst template provided the best fit. From these fits we find  $z_{\text{phot}} = 1.11 \pm 0.06 \pm 0.10 \pm 0.21$  (68%, 90%, and 99% confidence levels, respectively). In this case the Balmer jump is well sampled by the observations.

The photometric redshift determination has a well defined minimum at  $z \approx 1.1$  as shown in Fig. 2. The best fit values for the extinction, age, and redshifts are consistent independently of the extinction curve or template used. Using the observed template spectra from Kinney et al. (1996) give consistent results for the photometric redshift and extinction. Including also the HST bands in the SED fit, the resulting parameters ( $M_B$ , age,  $A_V$ ) do not change. Specifically  $z_{\text{phot}}$  does not change at all, but the uncertainty for the photometric redshift decreases by  $\sim 50\%$ . However, including the HST photometry increases the  $\chi^2$ . A fit when including the *LP* band gives  $\chi^2/\text{d.o.f.} = 1.315$ , while including the *CL* as well gives  $\chi^2/\text{d.o.f.} = 2.850$ . The reason for this is the calculation

TABLE 3  
SOLAR METALLICITY SED FITS

IMF	ext. law	$z_{\text{phot}}$ (68%, 99%)	$A_V$ (mag)	$\chi^2/\text{d.o.f.}$
Sp55	Cal00	$1.11^{+0.06, +0.21}_{-0.04, -0.18}$	0.20	0.399
MiSc79	Cal00	$1.11^{+0.06, +0.20}_{-0.06, -0.22}$	0.10	0.661
Sp55	SMC	$1.11^{+0.07, +0.23}_{-0.03, -0.45}$	0.12	0.427
MiSc79	SMC	$1.11^{+0.06, +0.21}_{-0.05, -0.21}$	0.06	0.651
Sp55	LMC	$1.11^{+0.07, +0.23}_{-0.04, -0.46}$	0.16	0.426
MiSc79	LMC	$1.11^{+0.06, +0.21}_{-0.06, -0.22}$	0.08	0.664
Sp55	MW	$1.11^{+0.07, +0.24}_{-0.04, -0.17}$	0.14	0.432
MiSc79	MW	$1.11^{+0.06, +0.21}_{-0.05, -0.21}$	0.06	0.662

NOTE. — Template SED fits using a Salpeter or Miller & Scalo IMFs, and different extinction curves. A redshift step of  $\Delta z = 0.05$  was used in our SED fits. Only ground-based photometric points were included in the fits. The derived properties in terms of best fit template type (Starburst), redshift, age (0.36 Gyr),  $M_B = -20.25$ , and extinction are basically independent of the input parameters for the assumed IMF and extinction curve. A relative host luminosity  $L/L^* \approx 0.5$  is derived assuming  $M_B^* = -21$  mag.

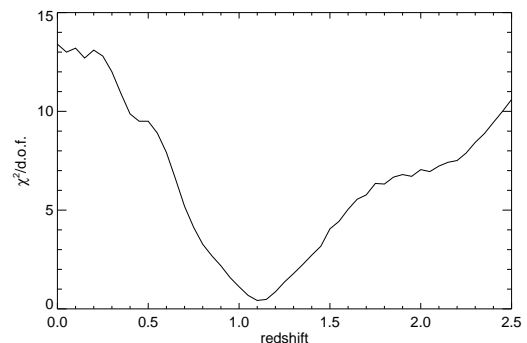


FIG. 2.— Reduced  $\chi^2$  as a function of redshift with a minimum at  $z \approx 1.11$  for the fit using the ground based data only.

of the effective wavelength of the two HST/STIS bands. In Fig. 2 the HST data points are shown by the squares.

We investigated whether using templates with metallicities different from solar values would have an impact on the output parameters. It is expected that the photometric redshift shows no significant difference while the well-known age-metallicity degeneracy would manifest itself. In Table 4 we list the results of fitting the observed SED with templates of metallicities of 0.2 and 0.4 solar, respectively. The template spectra were calculated using a Sp55 IMF with the GALAXEV code (Bruzual & Charlot 2003). Generally the best fit templates have larger ages, while the photometric redshifts are in good agreement with those in Table 3. Lower metallicities as well as templates constructed with a Chabrier (2003) IMF give consistent results for  $z_{\text{phot}}$ . Since all the fits give similar values of  $\chi^2$ , we can not disentangle this age-metallicity-extinction degeneracy using broad-band measurements alone (see also Bolzonella et al. 2000).

To check for consistency we used the Bayesian photometric redshift code (Benítez 2000) to estimate the photometric redshift. This code uses empirical spectral templates for the fits (Coleman et al. 1980). Us-

TABLE 4  
SUB-SOLAR METALLICITY SED FITS.

$Z/Z_{\odot}$	$z_{\text{phot}}$ (68%,99%)	Age (Gyr)	$A_V$ (mag)	$\chi^2/\text{d.o.f.}$
0.2	$1.11^{+0.09,+0.27}_{-0.06,-0.22}$	0.72	0.00	0.476
0.4	$1.11^{+0.06,+0.23}_{-0.05,-0.21}$	0.51	0.16	0.399

NOTE. — Here a Sp55 IMF and a Calzetti extinction law is used for creating the template. Only ground-based photometric points were used in the fits.

ing the same ground-based photometric points as above we find  $z_{\text{phot,BPZ}} = 0.94 \pm 0.13$  ( $\chi^2/\text{d.o.f.} = 1.078$ ), which is consistent with the results from HyperZ within  $1\sigma$  uncertainties. Including the HST data points gives  $z_{\text{phot,BPZ}} = 0.97 \pm 0.13$  ( $\chi^2/\text{d.o.f.} = 2.457$ ). The uncertainties reported here are  $1\sigma$  levels.

#### 4. DISCUSSION

Based on multi-colour optical and near-IR photometry we have reported the first precise photometric redshift for a GRB host galaxy without a spectroscopic redshift. The host is sufficiently bright that the prospects of obtaining a spectroscopic redshift, confirming or refuting our proposed value, appear feasible. We note however that we have been unable to detect emission lines in public VLT spectra in the ESO archive. In this connection it is interesting to note the relatively large mean age of the GRB 981226 host galaxy. This may indicate that emission lines are not prominent in this galaxy and reminds us that GRB host samples with spectroscopic redshifts may be biased towards emission line galaxies. The VLT spectra were obtained at a relatively low resolution ( $>10 \text{ \AA}$ ), and higher resolution data should be obtained to test the photometric redshift. At  $z \approx 1$  the optical emission lines could well be contaminated by residuals from subtraction of the skylines. Instruments such as ESI, MIKE, or the next generation instrument X-shooter could reveal such cases.

In addition to the photometric redshift, the SED also allows us to infer physical properties of the host galaxy. Assuming a redshift  $z = 1.11$  and the currently favored flat cosmology with  $\Omega_m = 0.3$  and  $H_0 = 70 \text{ km s}^{-1} \text{ Mpc}^{-1}$ , the luminosity distance is  $2.3 \times 10^{28} \text{ cm}$ . By interpolating a power law function between the observed  $B$  and  $R$  band AB magnitudes (corrected for extinction), we find that the rest frame 2800  $\text{\AA}$  Ultra Violet (UV) flux is  $0.27 \pm 0.06 \mu\text{Jy}$ . This corresponds to a star-formation rate (SFR) of  $1.2 \pm 0.3 \text{ M}_{\odot} \text{ yr}^{-1}$  using the

conversion between UV flux and a global SFR (Kennicutt 1998). The absolute magnitude of the host galaxy is  $M_B = -20.25 \text{ mag}$ , which implies a specific SFR of  $2.4 \pm 0.6 \text{ M}_{\odot} \text{ yr}^{-1} (L/L^*)^{-1}$ , where  $L^*$  corresponds to the luminosity of a galaxy with  $M_B^* = -21 \text{ mag}$ . This specific star formation rate is smaller than the UV based SFRs in a sample of 10 GRB hosts (Christensen et al. 2004a). As for other GRBs there is no indication that the host galaxy is strongly affected by extinction.

GRB 981226 had the interesting properties of being consistent with being both an almost-dark GRB (Jakobsson et al. 2004) and an X-ray flash (Frontera et al. 2000)<sup>3</sup>. We can use the inferred  $z_{\text{phot}}$  to estimate the peak energy for the BeppoSAX burst. Integrating a Band function and adding four power law functions to represent the X-ray to  $\gamma$ -ray spectrum at different time segments with the parameters given in Frontera et al. (2000), the total time integrated fluence is  $1.9 \times 10^{-6} \text{ erg cm}^{-2}$  and at  $z = 1.11$  the isotropic energy release is  $E_{\text{iso}} = 5.9 \times 10^{51} \text{ erg}$ . Frontera et al. (2000) divided the light curve into 5 segments, one of which had  $E_{\text{peak}}^{\text{obs}} = 61 \pm 15 \text{ keV}$ , the others less than 10 keV. The Amati relation (Ghirlanda et al. 2004a) predicts  $E_{\text{peak}} = 77.6 \text{ keV}$  and  $E_{\text{peak}}^{\text{obs}} = 36.9 \text{ keV}$ , consistent within  $2\sigma$  with the BeppoSAX observations of the peak energy. With small uncertainties in the luminosity distances, accurate photometric redshifts for other GRB hosts will help to constrain cosmological parameters through the Ghirlanda relation. The photometric redshift is higher than those reported for other XRFs but still lower than the median redshifts for GRBs, consistent with the hypothesis that XRFs may be off-axis GRBs or dirty fireballs which both predict lower mean redshifts.

We are very indebted to Dr. E. Harlaftis ( $\dagger$  2005 Feb 13) who took some of the VLT optical images analysed in this paper. We thank Dr. Micol Bolzonella for assistance with HyperZ. The authors acknowledge benefits from collaboration within the EU FP5 Research Training Network “Gamma Ray Bursts: An Enigma and a Tool”. L. Christensen acknowledges support by the German Verbundforschung associated with the ULTROS project, grant no. 05AE2BAA/4. The Dark Cosmology Centre is supported by the DNRF. The research of J. Gorosabel is partially supported by the Spanish Ministry of Science and Education through programmes ESP2002-04124-C03-01 and AYA2004-01515 (including FEDER funds).

$E_{\text{peak}} = 148 \pm 28 \text{ keV}$  reported in Ghirlanda et al. (2004b) refers to the BATSE burst.

#### REFERENCES

- Benítez, N. 2000, ApJ, 536, 571  
 Bloom, J. S., Gal, R. R., & Meltzer, J. 1998, GRB Circular Network, 182  
 Bloom, J. S., Kulkarni, S. R., & Djorgovski, S. G. 2002, AJ, 123, 1111  
 Bolzonella, M., Miralles, J.-M., & Pelló, R. 2000, A&A, 363, 476  
 Bruzual, A. G., & Charlot, S. 1993, ApJ, 405, 538  
 —. 2003, MNRAS, 344, 1000  
 Calzetti, D., Armus, L., Bohlin, R. C., Kinney, A. L., Koornneef, J., & Storchi-Bergmann, T. 2000, ApJ, 533, 682  
 Castro-Tirado, A. J. et al. 1998, GRB Circular Network, 173  
 Chabrier, G. 2003, PASP, 115, 763  
 Christensen, L., Hjorth, J., & Gorosabel, J. 2004a, A&A, 425, 913  
 Christensen, L., Hjorth, J., Gorosabel, J., Vreeswijk, P., Fruchter, A., Sahu, K., & Petro, L. 2004b, A&A, 413, 121

- Coleman, G. D., Wu, C.-C., & Weedman, D. W. 1980, *ApJS*, 43, 393
- Fitzpatrick, E. L. 1986, *AJ*, 92, 1068
- Frail, D. A. et al. 1999, *ApJL*, 525, L81
- Frontera, F. et al. 2000, *ApJ*, 540, 697
- Galama, T. J., et al. 1998, GRB Circular Network, 172
- Gehrels, N. et al. 2004, *ApJ*, 611, 1005
- Ghirlanda, G., Ghisellini, G., & Lazzati, D. 2004a, *ApJ*, 616, 331
- Ghirlanda, G., Ghisellini, G., & Celotti, A. 2004b, *A&A*, 422, L55
- Gorosabel, J. et al. 2003a, *A&A*, 400, 127
- . 2003b, *A&A*, 409, 123
- Gorosabel, J. et al. 2005, *A&A* in press (astro-ph/0507488)
- Holland, S. 2000, GRB Circular Network, 749
- Holland, S. 2001, in *AIP Conf. Proc.* 586: 20th Texas Symposium on relativistic astrophysics, 593
- Jakobsson, P., Hjorth, J., Fynbo, J. P. U., Watson, D., Pedersen, K., Björnsson, G., & Gorosabel, J. 2004, *ApJ*, 617, L21
- Jakobsson, P. et al. 2005, *MNRAS* in press (astro-ph/0505542)
- Kennicutt, R. C. 1998, *ARA&A*, 36, 189
- Kinney, A. L., Calzetti, D., Bohlin, R. C., McQuade, K., Storchi-Bergmann, T., & Schmitt, H. R. 1996, *ApJ*, 467, 38
- Klose, S. 1998, GRB Circular Network, 186
- Le Floc'h, E. et al. 2003, *A&A*, 400, 499
- Lindgren, B. et al. 1999, GRB Circular Network, 190
- Miller, G. E., & Scalo, J. M. 1979, *ApJS*, 41, 513
- Prevot, M. L., Lequeux, J., Prevot, L., Maurice, E., & Rocca-Volmerange, B. 1984, *A&A*, 132, 389
- Rhoads, J., Orosz, J. A., Lee, J., & Stassun, K. 1998, GRB Circular Network, 181
- Rol, E., Wijers, R. A. M. J., Kouveliotou, C., Kaper, L., & Kaneko, Y. 2005, *ApJ*, 624, 868
- Salpeter, E. E. 1955, *ApJ*, 121, 161
- Schaefer, B. E., Kemp, J., Feygina, I., & Halpern, J. 1998, GRB Circular Network, 185
- Schlegel, D. J., Finkbeiner, D. P., & Davis, M. 1998, *ApJ*, 500, 525
- Seaton, M. J. 1979, *MNRAS*, 187, 73P
- Taylor, G. B., Frail, D. A., Kulkarni, S. R., Shepherd, D. S., Feroci, M., & Frontera, F. 1998, *ApJ*, 502, L115
- Wozniak, P. R. 1998, GRB Circular Network, 177